

Birth of strange nonchaotic attractors in a piecewise linear oscillator

Cite as: Chaos **32**, 103106 (2022); <https://doi.org/10.1063/5.0096959>

Submitted: 23 April 2022 • Accepted: 08 September 2022 • Published Online: 10 October 2022

Jicheng Duan,  Wei Zhou,  Denghui Li, et al.



View Online



Export Citation



CrossMark

ARTICLES YOU MAY BE INTERESTED IN

[Abrupt transition of the efficient vaccination strategy in a population with heterogeneous fatality rates](#)

Chaos: An Interdisciplinary Journal of Nonlinear Science **32**, 093140 (2022); <https://doi.org/10.1063/5.0087627>

[Simplicial epidemic model with birth and death](#)

Chaos: An Interdisciplinary Journal of Nonlinear Science **32**, 093144 (2022); <https://doi.org/10.1063/5.0092489>

[Network spreading among areas: A dynamical complex network modeling approach](#)

Chaos: An Interdisciplinary Journal of Nonlinear Science **32**, 103102 (2022); <https://doi.org/10.1063/5.0102390>

APL Machine Learning

Open, quality research for the networking communities

Now Open for Submissions

LEARN MORE

Birth of strange nonchaotic attractors in a piecewise linear oscillator

Cite as: Chaos 32, 103106 (2022); doi: 10.1063/5.0096959

Submitted: 23 April 2022 · Accepted: 8 September 2022 ·

Published Online: 10 October 2022



View Online



Export Citation



CrossMark

Jicheng Duan,¹ Wei Zhou,^{2,a)} Denghui Li,³ and Celso Grebogi⁴

AFFILIATIONS

¹School of Mathematics and Physics, Lanzhou Jiaotong University, Lanzhou, Gansu 730070, China

²Institute of Decision and Game Theory, Lanzhou Jiaotong University, Lanzhou, Gansu 730070, China

³School of Mathematics and Statistics, Hexi University, Zhangye, Gansu 734000, China

⁴Institute for Complex Systems and Mathematical Biology King's College, University of Aberdeen, Aberdeen AB24 3UE, United Kingdom

^{a)}Author to whom correspondence should be addressed: wei_zhou@vip.126.com

ABSTRACT

Nonsmooth systems are widely encountered in engineering fields. They have abundant dynamical phenomena, including some results on the complex dynamics in such systems under quasiperiodically forced excitations. In this work, we consider a quasiperiodically forced piecewise linear oscillator and show that strange nonchaotic attractors (SNAs) do exist in such nonsmooth systems. The generation and evolution mechanisms of SNAs are discussed. The torus-doubling, fractal, bubbling, and intermittency routes to SNAs are identified. The strange properties of SNAs are characterized with the aid of the phase sensitivity function, singular continuous spectrum, rational frequency approximation, and the path of the partial Fourier sum of state variables in a complex plane. The nonchaotic properties of SNAs are verified by the methods of maximum Lyapunov exponent and power spectrum.

Published under an exclusive license by AIP Publishing. <https://doi.org/10.1063/5.0096959>

Strange nonchaotic attractors (SNAs) can be regarded as a special class of attractors between quasiperiodic attractors and chaotic attractors. The word strange means that the dependence of the dynamical variables to the phase is not given by the smooth relations but constitutes some fractal ones. The word nonchaotic means that the maximum Lyapunov exponent is nonpositive. However, there are few studies on SNAs in nonsmooth dynamical systems. In this work, we study a quasiperiodically forced piecewise linear oscillator. The complicated and interesting strange nonchaotic dynamics phenomena are revealed via numerical methods.

I. INTRODUCTION

SNAs have a geometric fractal structure, but the maximum Lyapunov exponent is nonpositive, which exhibits nonchaotic properties in a dynamic sense. Since SNAs were uncovered by Grebogi *et al.*,¹ it was realized that strangeness is not equivalent to chaos. SNAs have been widely studied experimentally and numerically. Ding *et al.*² confirmed the existence of SNAs from numerical and

analytical methods and illustrated various dynamical behaviors in a typical quasiperiodically forced system. Pikovsky and Feudel³ described strange properties of such attractors by calculating the phase sensitivity exponents. With the aid of a function equation for the invariant curve, Nishikawa and Kaneko⁴ studied the fractal structure and chaotic evolution of a class of SNAs in a quasiperiodically forced logistic map. Ditto *et al.*⁵ observed SNAs in a two-frequency quasiperiodically driven, buckled, magnetoelastic ribbon experiment. According to an experiment and numerical simulation, Thamilmaran *et al.*⁶ identified chaotic attractors and SNAs in a circuit system and distinguished these two kinds of attractors by the Poincaré map, maximum Lyapunov exponents, and their variance. In addition, Linder *et al.*⁷ established the existence of strange nonchaotic stars through the Kepler space telescope, which further indicates the presence of strange nonchaotic phenomena in nature.

The mathematical research of SNAs mainly focused on skew product systems (see, e.g., Refs. 8–10). Keller¹¹ investigated a class of skew product maps that have monotonically increasing and strictly concave fiber maps. It was proved that the system has an attracting invariant curve, which is almost everywhere discontinuous and, thus, an SNA. Ding *et al.*¹² and Fuhrmann *et al.*¹³ studied the

fractal dimension of SNAs in the quasiperiodically forced monotone interval maps, which are created through nonsmooth saddle-node bifurcation, and determined that the Hausdorff dimension and box-counting dimension have different values. Other theoretical results of SNAs are about discrete Schrödinger equation with quasiperiodic potential in which the Harper map is a typical example. Haro and Puig¹⁴ proved that the Harper map has SNAs in a set of parameter values of positive Lebesgue measure. These proofs involved spectrum analysis of the Schrödinger operator and the estimate of the Lyapunov exponent.

Although the existence of SNAs has been studied widely in quasiperiodically forced systems (cf. Refs. 15–18), there are still many interesting questions, for instance: how SNAs are generated and eventually evolve into chaotic attractors? Precisely, what exactly causes SNAs is somewhat vague since the bifurcation mechanisms of quasiperiodic driving systems have not been understood in detail. However, several routes to SNAs have been described in the literature, such as Heagy–Hammel route,^{19,20} fractal route,²¹ intermittency route,^{22,23} Blowout bifurcation route,²⁴ and so on. The literature offers overviews and further references for other routes (see, e.g., Refs. 25–29).

The studies of SNAs are mainly limited to smooth systems. The mechanism of SNA generation is more complicated in nonsmooth systems since there exist many nontypical bifurcations, such as grazing bifurcation, sliding bifurcation, period-adding bifurcation, and so on. Li *et al.*³⁰ studied a piecewise smooth map quasiperiodically forced and found three routes (Heagy–Hammel route, fractal route, and type-I intermittency route) to SNAs in the parameter space. Shen and Zhang³¹ revealed several types of routes to SNAs in two critical tongue-type regions in a quasiperiodically forced piecewise logistic map. Zhang *et al.*³² studied a class of quasiperiodically forced interval maps and showed that smooth quasiperiodic torus attractors lose their smoothness by grazing bifurcation and eventually become SNAs. Li *et al.*³³ discovered that SNAs exist between two parameter regions corresponding to chaotic motions and further discussed the coexistence of SNAs, quasiperiodic attractors, and chaotic attractors in a nonsmooth mechanical system.

The piecewise linear systems are a class of classical nonsmooth dynamical systems.^{34–36} There are still only a few results about the complex dynamics in such systems with quasiperiodic excitations. In this work, we identify and analyze the existence of SNAs in a piecewise linear oscillator with quasiperiodic force, and the dynamics transition of the system is further discussed. The remaining of this paper is organized as follows. In Sec. II, we briefly describe the mathematical model of the piecewise linear oscillator and its Poincaré map. Then, the doubling and period-adding phenomena of the dynamics are investigated in Sec. III. The generation and existence mechanisms of SNAs are discussed in Sec. IV. The main results are summarized in Sec. V.

II. THE PIECEWISE LINEAR OSCILLATOR WITH QUASIPERIODIC EXCITATION AND ITS POINCARÉ MAP

Consider a piecewise linear oscillator shown in Fig. 1. The mass m is attached to a linear spring of stiffness k_1 and a damper of damping coefficient c_1 . It is being acted upon by a quasiperiodic

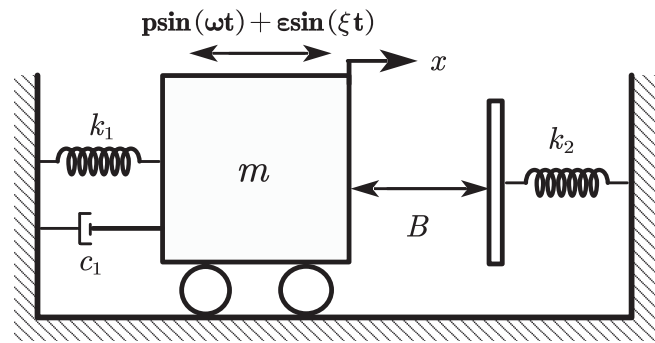


FIG. 1. The piecewise linear oscillator.

force $p \sin(\omega t) + \varepsilon \sin(\xi t)$. When the displacement x exceeds a certain value B , the second linear spring with stiffness k_2 contacts the mass m .

The differential equation of motion of the system can be expressed as

$$m\ddot{x} + c_1\dot{x} + K(x) = p \sin(\omega t) + \varepsilon \sin(\xi t), \quad (1)$$

where

$$K(x) = \begin{cases} k_1x & \text{if } x \leq B, \\ k_1x + k_2(x - B) & \text{if } x > B. \end{cases} \quad (2)$$

Let $\theta = \omega t, \phi = \xi t$. Then, Eq. (1) can be written in the following form:

$$\begin{cases} \dot{x} = v, \\ \dot{v} = (-c_1v - K(x) + p \sin(\theta) + \varepsilon \sin(\phi))/m, \\ \dot{\phi} = \xi, \\ \dot{\theta} = \omega. \end{cases} \quad (3)$$

A stroboscopic section is taken in each period $2\pi/\xi$. We obtain the following Poincaré map of the system (3), which has the form

$$\begin{aligned} x_{n+1} &= f_1(x_n, v_n, \theta_n), \\ v_{n+1} &= f_2(x_n, v_n, \theta_n), \\ \theta_{n+1} &= \theta_n + \frac{2\pi}{\xi} \pmod{2\pi}, \end{aligned} \quad (4)$$

where f_1 and f_2 are determined by (3).

III. THE DOUBLING AND PERIOD-ADDING PHENOMENA IN THE DYNAMICS

A. The bifurcations in the unperturbed system

In order to understand the dynamical behavior of system (3), we first consider the unperturbed system, i.e., the case $\varepsilon = 0$. The bifurcation diagram of the unperturbed system by varying the external excitation frequency ω is shown in Figs. 2(a) and 2(b), where the other parameter values are $p = 10, m = 0.5, k_1 = 1.0, k_2 = 30, c_1 = 0.2, B = 0.0001$, and the initial values are $(x_0, v_0, \theta_0, \phi_0) = (0, 0, 0, 0)$.

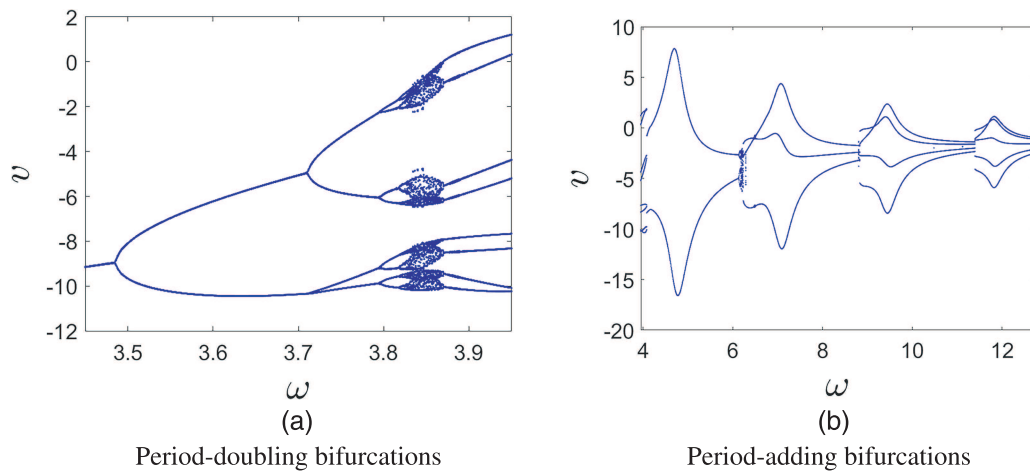


FIG. 2. The bifurcation diagram of the unperturbed system with respect to the parameter ω . (a) Period-doubling bifurcations. (b) Period-adding bifurcations.

When the bifurcation parameter $\omega = 3.486$, the system has the first period-doubling bifurcation and the corresponding Floquet multipliers of the system are $\lambda_1 = -1$ and $\lambda_2 = -0.486$, where $\lambda_1 = -1$ goes through $(-1, 0)$ on the unit circle, and the absolute value of another eigenvalue $|\lambda_2| = 0.486 < 1$ is still inside the unit circle. As ω increases to 3.712, the system has the second period-doubling bifurcation which converts the attractor from period-2 to period-4. For $\omega = 3.797$, the period-4 attractor evolves into a period-8 attractor. After a series of period-doubling bifurcations, the system evolves into chaos. When ω is greater than 3.868, the system again returns to periodic motion with a period-8 attractor [see Fig. 2(a)]. In addition, there are period-adding bifurcations in the unperturbed system [see Fig. 2(b)].

B. The torus-doubling of the system with quasiperiodic excitation

For system (3), we take $\xi = (\sqrt{5} - 1)/2$, since ξ is the inverse of the golden ratio, the dynamics along the θ -axis is ergodic, and the trajectory for every initial condition uniformly covers the θ -axis. We take the frequency ω as the control parameter, varying between 3.45 and 3.6. The amplitude $\varepsilon = 0.3$, the other parameter values, and the initial values are the same as in Sec. III A. The maximum Lyapunov exponent varying with the parameter ω is shown in Fig. 3, where $1T, 2T$, and $4T$ correspond to torus, doubled torus, and torus of period-4, respectively. In system (3), SNAs do exist between quasiperiodic motion and chaotic motion. With the aid of the maximum Lyapunov exponent, we can distinguish the types of attractors in the given parameter interval. When the parameter $\omega \in [3.45, 3.562]$, the system exhibits quasiperiodic motion. We select the interval $(3.562, 3.565)$ as the candidate interval for the existence of SNAs. In Sec. IV, we will further verify that this interval is corresponding to SNAs through the Lyapunov exponent, phase diagrams, and phase sensitivity property. When the parameter $\omega \in [3.565, 3.6]$, the system exhibits chaotic motion, namely, the maximum Lyapunov exponent of the system is positive.

IV. STRANGE NONCHAOTIC ATTRACTORS

In this section, we use quantitative and qualitative methods to verify the existence of SNAs in system (3) and describe four scenarios for the birth of the SNAs from quasiperiodic behaviors.

We first introduce the power spectrum (Fourier amplitude spectrum), which is an effective tool to distinguish various types of attractors. In general, a dynamical system can manifest two types of power spectrum, namely, continuous and discrete spectrum. Discrete spectrum corresponds to the occurrence of oscillations at specific frequencies such as that of periodic or quasiperiodic oscillations. In contrast, the broadband nature of the frequency spectrum in the case of chaotic oscillations points toward continuous spectrum. For a special case like SNA, the spectrum exhibits a combination of both continuous and discrete components, known as

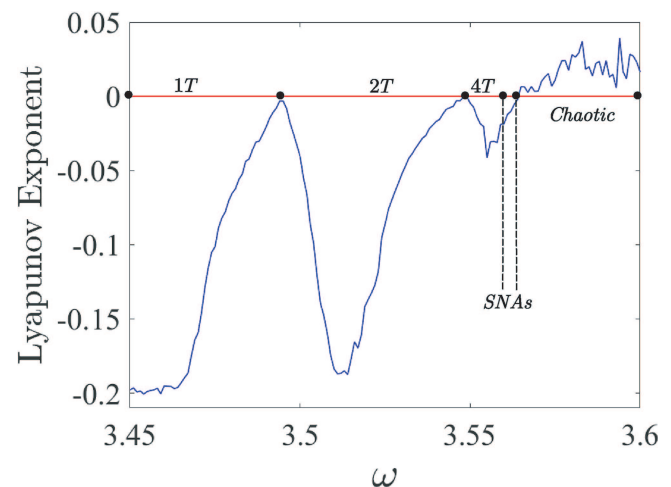


FIG. 3. The maximum Lyapunov exponent with the variation of ω for system (3).

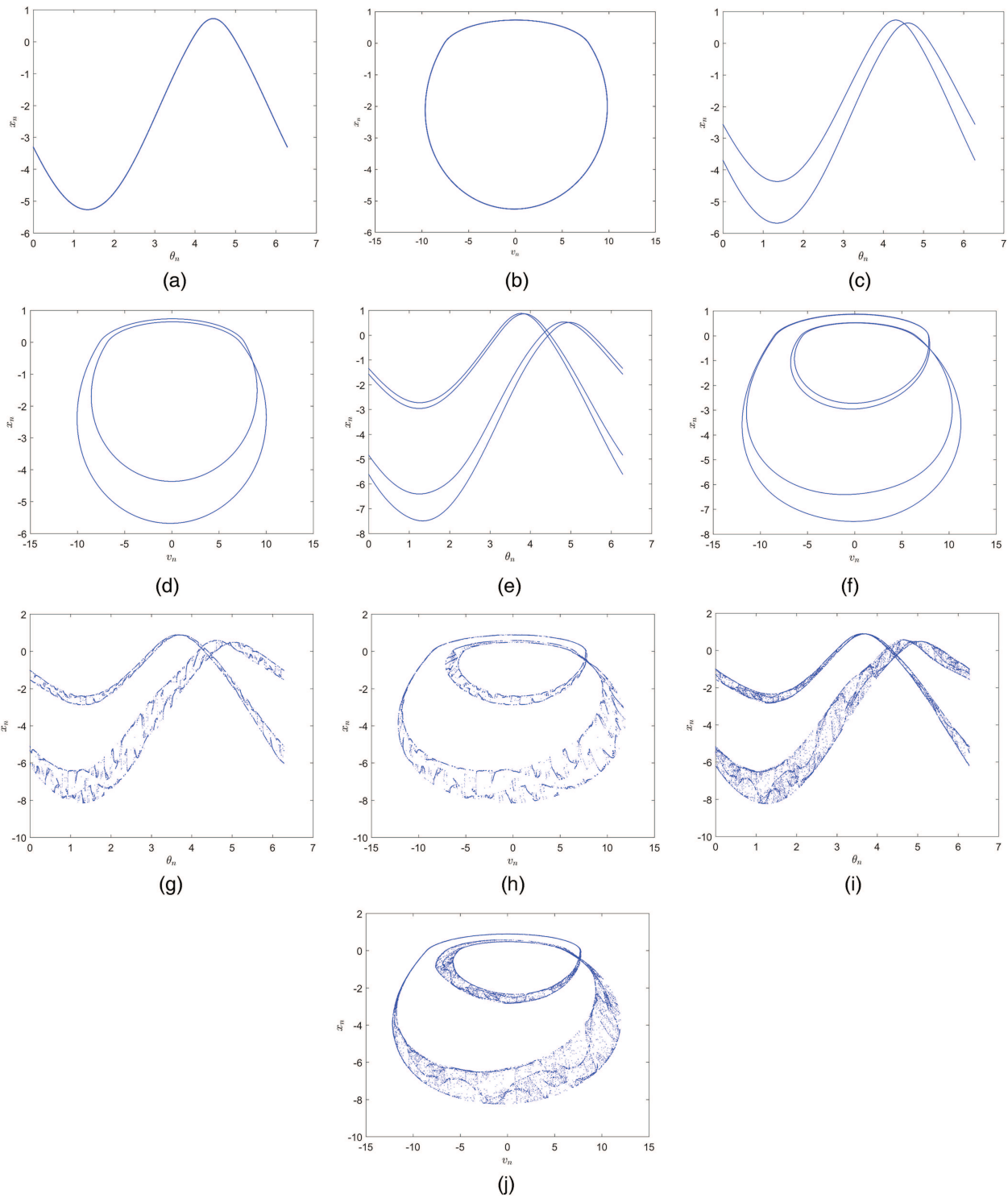


FIG. 4. For $\varepsilon = 0.3$, the phase diagrams of attractors in the (θ_n, x_n) -plane and (v_n, x_n) -plane: (a) and (b) $\omega = 3.45$, (c) and (d) $\omega = 3.5$, (e) and (f) $\omega = 3.551$, (g) and (h) $\omega = 3.5647$, (i) and (j) $\omega = 3.567$.

a singular continuous spectrum (cf. Ref. 37). We take the Fourier transform of the process $\{x_n\}$,

$$X(\Omega, T) = \sum_{n=1}^T x_n e^{i2\pi n\Omega}. \tag{5}$$

Hence, the power spectrum of the attractor is defined as³⁸

$$P_\Omega = \lim_{T \rightarrow \infty} |X(\Omega, T)/T|^2, \tag{6}$$

where Ω is proportional to the frequency ratio of the two excitation forces in the system.

A. The torus collision route

Torus collision is a generating mechanism of SNAs, which is closely related to period-doubling bifurcation. With the change of the control parameter ω , a stable 2^n T quasiperiodic attractor appears by torus-doubling bifurcation. The parent torus becomes unstable in the quasiperiodically driven system (the pitchfork bifurcation can take place in the system without driving force, that is, the unstable periodic 2^n orbit can form the periodic 2^{n+1} orbit). Hence, the stable 2^n T quasiperiodic attractor collides with its unstable parent torus to generate SNAs.

To clearly indicate the geometrically smooth or complicated structure of attractors, we can draw the phase diagrams of Poincaré section in the (θ_n, x_n) -plane with $\theta \bmod 2\pi$, and in (v_n, x_n) -plane, respectively. Figure 4 shows the evolution of typical attractors as ω varies and we can depict the creation of the SNAs by the torus-doubling. When $\omega = 3.45$, the attractor is quasiperiodic in the Poincaré sections, and the system exhibits an invariant torus in the (v_n, x_n) -plane, namely, a 1 T quasiperiodic attractor occurs [see Figs. 4(a) and 4(b)]. As ω increases, for example, $\omega = 3.5$, the attractor becomes a two-tori (2T) quasiperiodic attractor and the invariant curve becomes two smooth curves, which are created by a torus-doubling bifurcation from the period-1 repeller [see Figs. 4(c) and 4(d)]. When ω passes through 3.548, the torus-doubling bifurcation occurs again, and the 2 T quasiperiodic attractor evolves into a 4 T quasiperiodic attractor [see Figs. 4(e) and 4(f)]. In general,

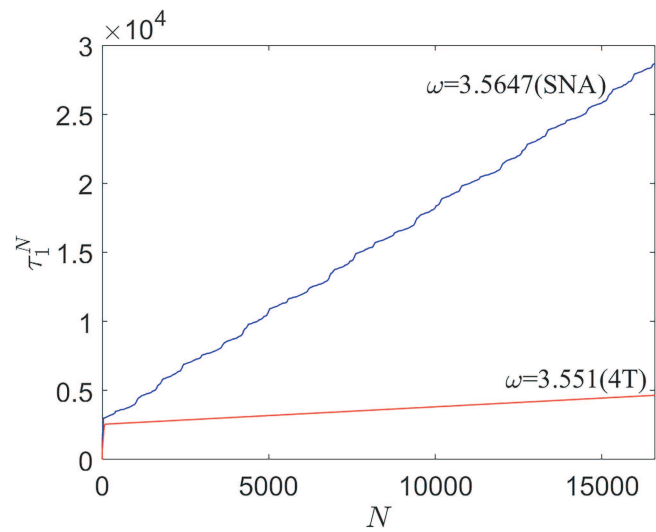


FIG. 5. The phase sensitivity exponent τ_1^N vs N , the 4T for $\omega = 3.551$ (red line) and SNA for $\omega = 3.5647$ (blue line).

the torus-doubling continues indefinitely until a critical point is reached beyond which the system exhibits chaotic motion. However, as ω increases further to 3.5647, the 4 T quasiperiodic attractor collides with its unstable parent torus; hence, the attractor becomes extremely wrinkled, loses its smoothness, and results in a strange attractor. This is reflected in Figs. 4(g) and 4(h), which indicate the apparent discontinuity in the Poincaré map and the doubling of the torus is interrupted. During this process, the maximum Lyapunov exponent remains negative ($\lambda \approx -0.00203$), which is shown in Fig. 3. Therefore, we conclude that the system is in the strange nonchaotic state for $\omega = 3.5647$. Finally, the attractor deforms and the SNA becomes larger and forms a chaotic attractor with $\omega = 3.567$ [see Figs. 4(i) and 4(j)].

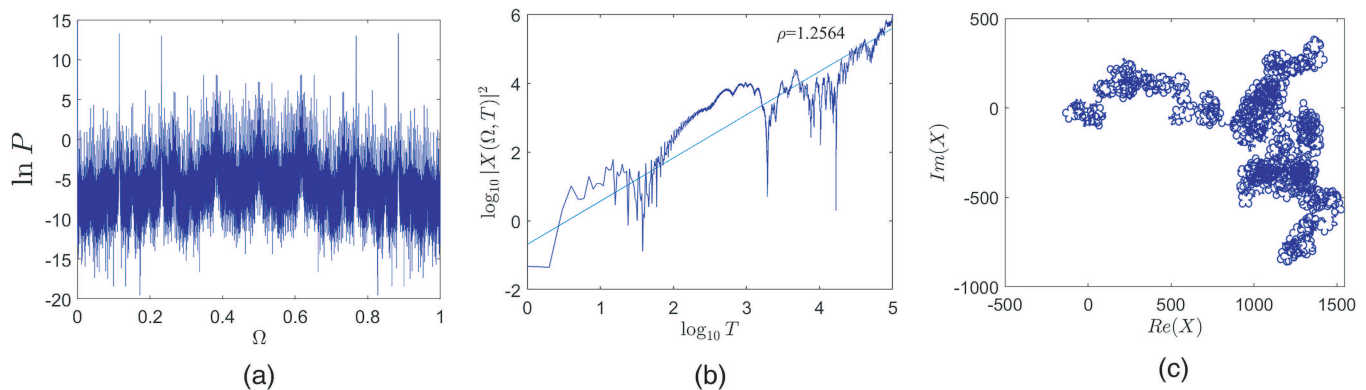


FIG. 6. For $\omega = 3.5647$. (a) The singular continuous spectrum. (b) The finite-time Fourier spectrum $X(\Omega, T)$ vs T in logarithmic scale. (c) The fractal walk in the complex plane (ReX, ImX).

B. Check the strange properties of attractors

In Secs. I–III, we studied the evolution of the attractors with the help of phase diagram and power spectrum and verified the nonchaotic characteristics of SNAs by the maximum Lyapunov exponent. To further illustrate the strange properties of the attractor, we will use the phase sensitivity function, singular continuous spectrum, and rational approximation method.

1. Phase sensitivity property

If the attractor is regarded as a fractal curve, then its nondifferentiability can be detected by the phase sensitivity. This method is based on the sensitivity of the attractor to the phase of the external excitation. There are some special tangent bifurcation points in SNAs, where the derivative of these bifurcation points with respect to the phase is infinite, and the tangent is orthogonal to the θ -axis, showing that the attractor is nonsmooth. The derivative with respect

to the external phase can be denoted as (cf. Ref. 3)

$$S_i(N) = \frac{\partial f_i}{\partial \theta} (i = 1, 2), \tag{7}$$

where N is the number of iterations. If $S_i(N)$ tends to be infinite as $N \rightarrow \infty$, the attractor is nonsmooth, which means that the attractor is strange.

The phase sensitivity can be calculated from the time series in the attractors. For any small ε , we can find n_0 to satisfy the phase difference $\varepsilon_0 = |\theta_{n_0} - \theta_0| < \varepsilon$, and the $S_i(N)$ can be approximately expressed as

$$\begin{aligned} S_i(N) &= \frac{\partial f_i}{\partial \theta} \approx \sum_{k=1}^{N-n_0} \left| \frac{f_i(k+n_0) - f_i(k)}{\theta(k+n_0) - \theta(k)} \right| \\ &= \sum_{k=1}^{N-n_0} \left| \frac{f_i(k+n_0) - f_i(k)}{\varepsilon_0} \right| (i = 1, 2), \end{aligned} \tag{8}$$

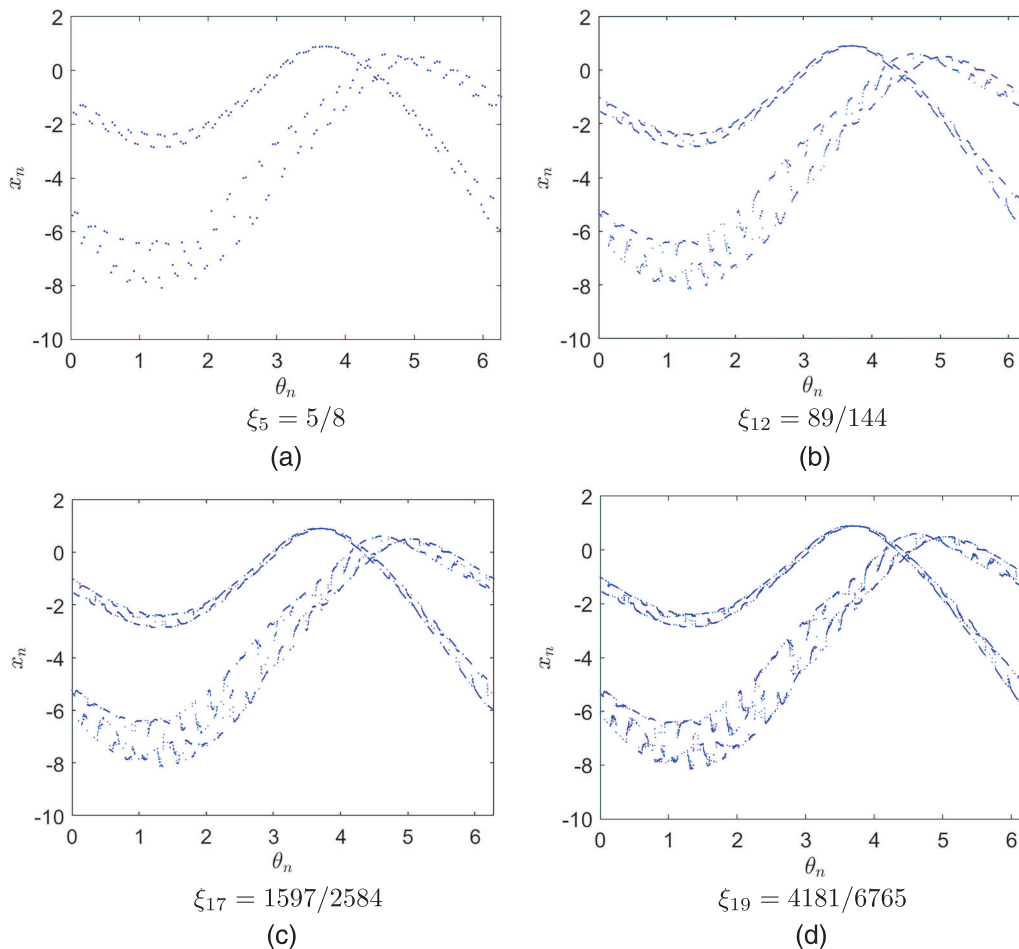


FIG. 7. The rational approximations of the SNA for $\omega = 3.5647$ in the (θ_n, x_n) -plane. (a) $\xi_5 = 5/8$, (b) $\xi_{12} = 89/144$, (c) $\xi_{17} = 1597/2584$, (d) $\xi_{19} = 4181/6765$.

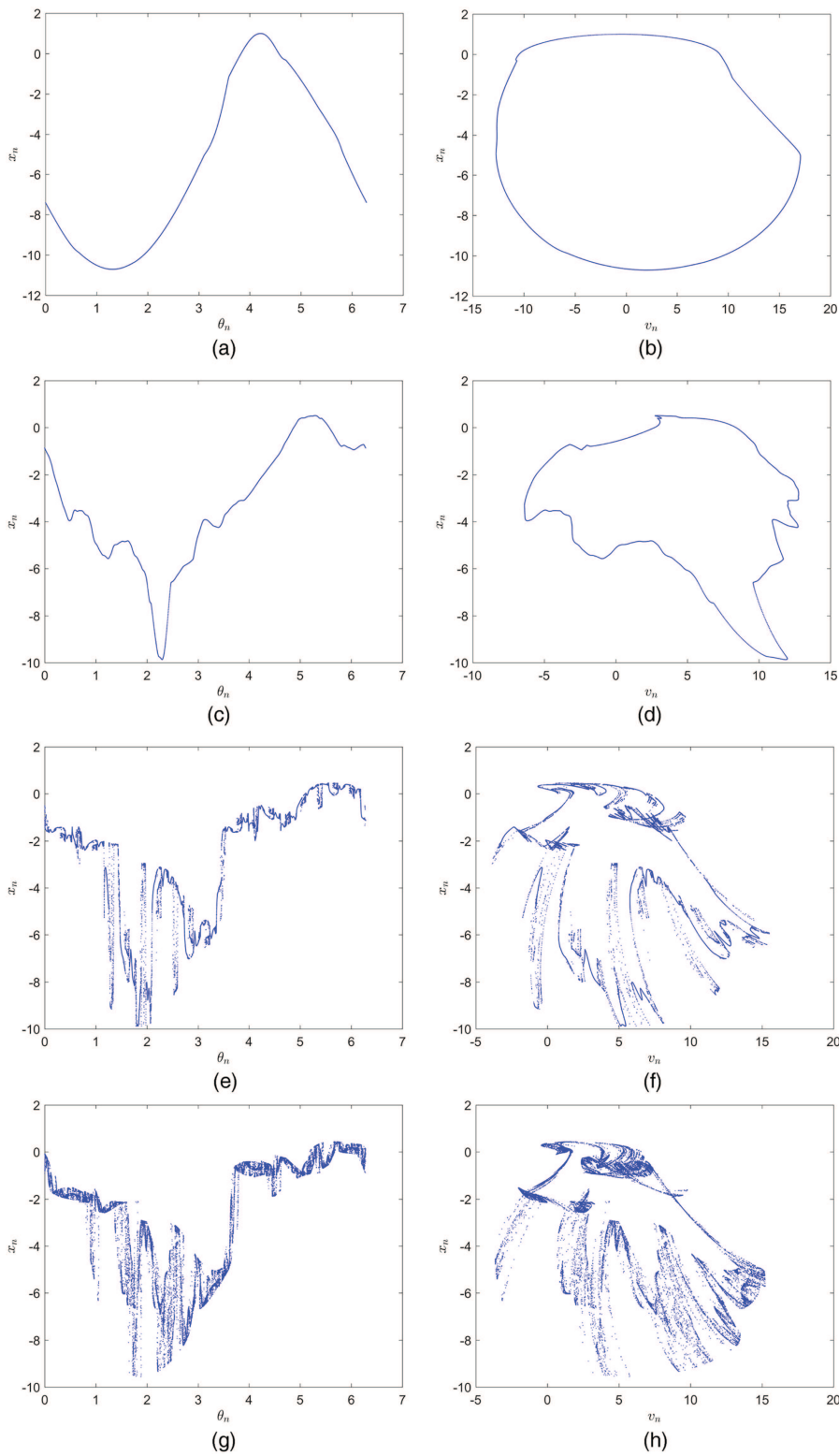


FIG. 8. For $\varepsilon = 3.1$, the phase diagrams of attractors in the (θ_n, x_n) -plane and (v_n, x_n) -plane: (a) and (b) $\omega = 3.2$, (c) and (d) $\omega = 3.38$, (e) and (f) $\omega = 3.43$, (g) and (h) $\omega = 3.44$.

where $k + n_0 \leq N$, and $f_i(k)$ denotes the k th iteration of f_i . The maximum value of $S_i(N)$ after N times iterations is denoted as

$$\tau_i^N = \max \{S_i(N)\}. \tag{9}$$

If the number of iterations increases, the value of τ_i^N increases gradually. Then, $S_i(N)$ tends to infinite as $N \rightarrow \infty$, which means that the attractor is strange.

We take two groups of parameter values to verify strange properties by phase sensitivity function. Let $n_0 = 4182$, then $|\theta(k + n_0) - \theta(k)| \equiv 0.000672$, when $\omega = 3.5647$, the value of τ_1^N tends to infinity as the number of iterations increases, which indicates that the attractor is strange. On the contrary, when $\omega = 3.551$, the value of τ_1^N does not increase with the increase of iterations, which indicates that the attractor is smooth (see Fig. 5).

2. Singular continuous spectrum

The strange properties of the attractor can be examined by means of the singular continuous spectrum. For $\omega = 3.5647$, the spectrum shows singular continuity [see Fig. 6(a)]. In general, $X(\Omega, T)$ and T have a power-law relationship (see Ref. 39 for details).

Let

$$|X(\Omega, T)|^2 \sim T^\rho, \tag{10}$$

where ρ is a scaling exponent. If an SNA exists, then $1 < \rho < 2$. When the system exhibits periodic or quasiperiodic motion, the corresponding scaling exponent is $\rho = 2$. If the system exhibits chaotic motion, the scaling exponent is $\rho = 1$. For the SNA in Fig. 4(g), the corresponding finite-time Fourier spectrum $X(\Omega, T)$ vs T in logarithmic scale is exhibited in Fig. 6(b), where we detect a relatively robust power-law behavior with $\rho = 1.2564$. In addition, $X(\Omega, T)$ defines a path in a complex plane (Re X , Im X) when T is regarded as time and a fractal self-similar path corresponds to $|X(\Omega, T)|^2 \sim T^{1.2564}$ [see Fig. 6(c)].

3. The rational approximation

The rational approximation is also an important method to determine the strange properties of SNAs, which is based on the fact that all irrational numbers can be approximated by appropriate rational numbers (cf. Ref. 3). When the approximation order is low, only some periodic points can be observed and the shape of

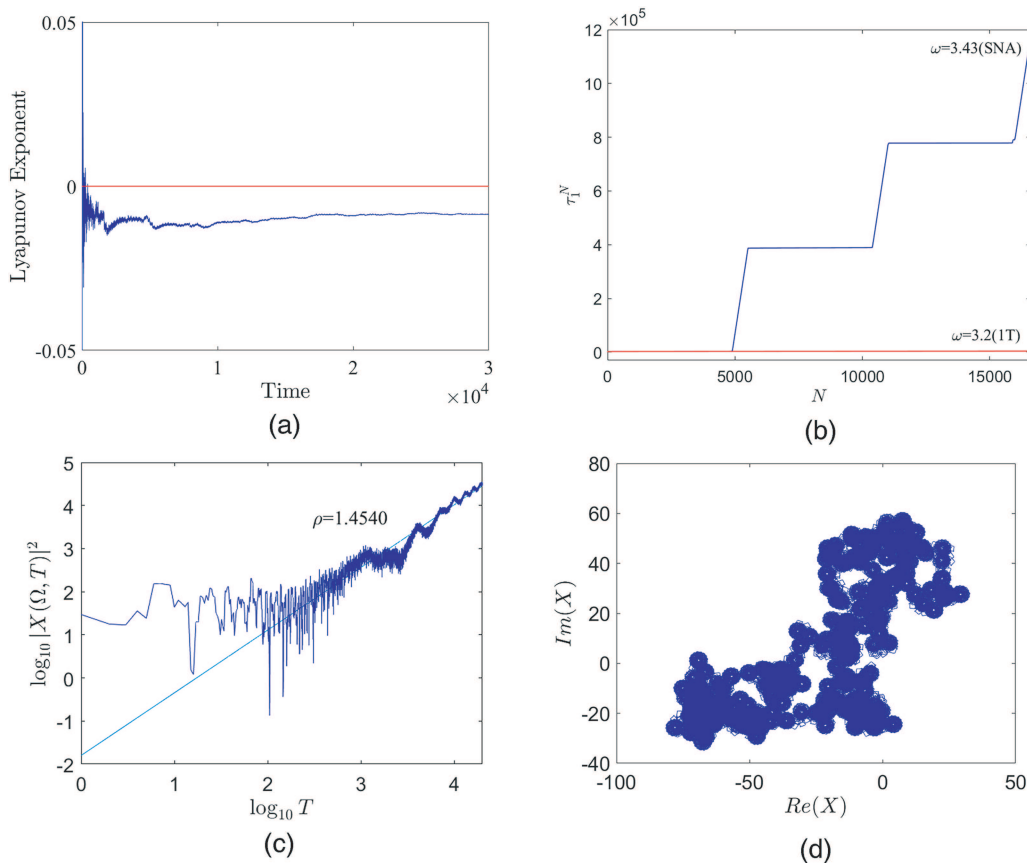


FIG. 9. For $\omega = 3.43$. (a) The maximum Lyapunov exponent. (b) The phase sensitivity exponent τ_1^N vs N , the 1T for $\omega = 3.2$ (red line) and SNA for $\omega = 3.43$ (blue line). (c) The finite-time Fourier spectrum $X(\Omega, T)$ vs T in logarithmic scale. (d) The fractal walk in the complex plane (Re X , Im X).

SNAs cannot be presented. As the order of approximation increases, the number of periodic points tends to infinite, and the structure of the attractor is not a finite set of points and is not piecewise differentiable, which depicts the strangeness of the attractor. In the following, we use rational numbers to approximate the frequency ξ , which is taken as $(\sqrt{5} - 1)/2$. The ratio ξ_k of the Fibonacci sequences can be used to approximate ξ , where $\xi_k = F_{k-1}/F_k$, $F_k = F_{k-1} + F_{k-2}$, $F_1 = 1, F_2 = 1$, and $\xi = \lim_{k \rightarrow \infty} \xi_k$. Take the

attractor in Fig. 4(j) as an example. Figures 7(a)–7(d) are the phase diagrams of the attractor in the (θ_n, x_n) -plane for different approximate orders k . In Fig. 7(a), only some periodic points can be observed when $\xi_5 = 5/8$. As k gradually increases, the number of periodic points gradually increases, and the fractal characteristics of the attractor gradually appear [Figs. 7(b) and 7(c)]. When $\xi_{19} = 4181/6765$, the number of periodic points becomes virtually uncountable, the attractor begins to appear nonsmoothly, and an

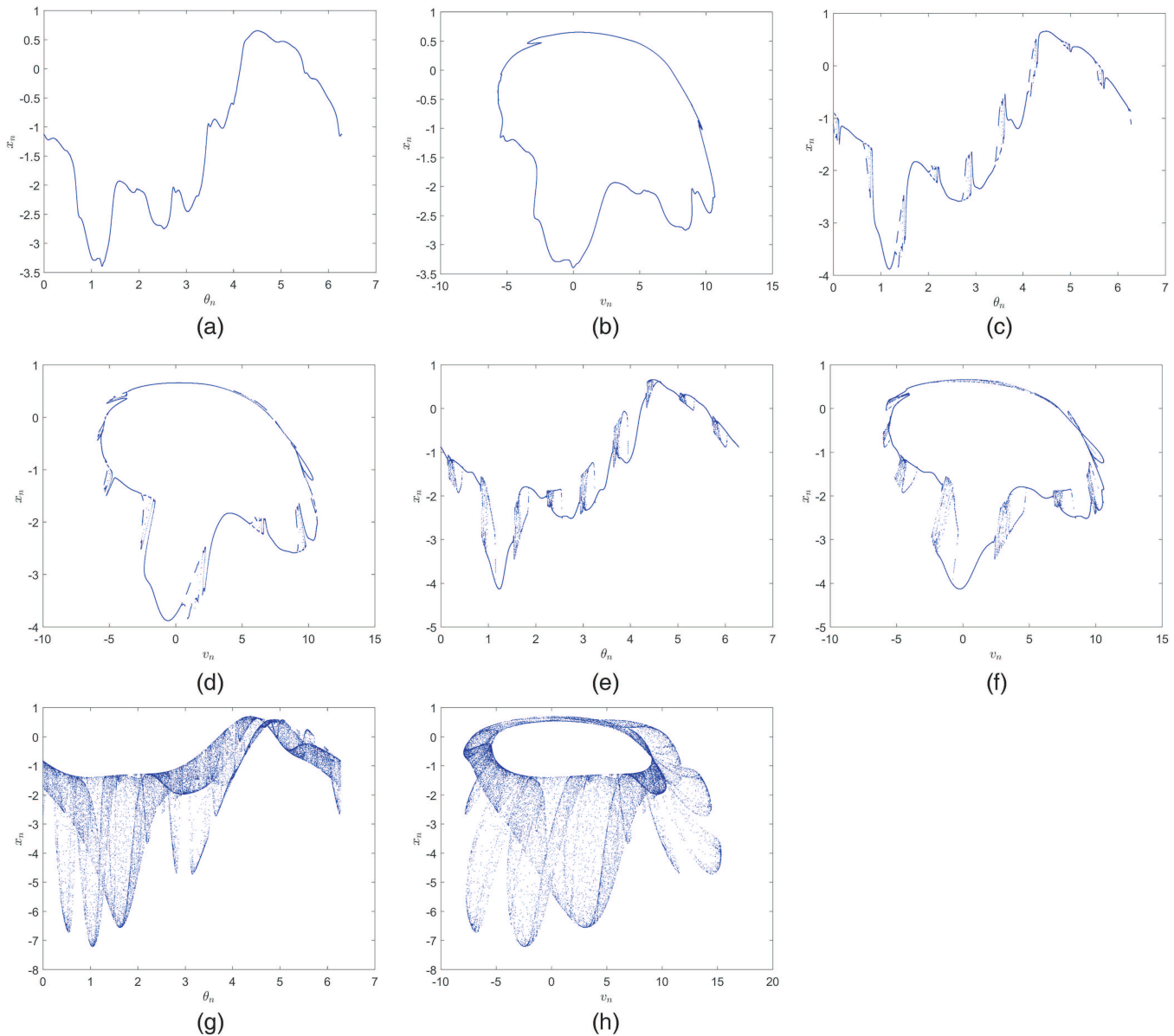


FIG. 10. For $\varepsilon = 1.5$, the phase diagrams of attractors in the (θ_n, x_n) -plane and (v_n, x_n) -plane: (a) and (b) $\omega = 3.363$, (c) and (d) $\omega = 3.3645$, (e) and (f) $\omega = 3.365$, (g) and (h) $\omega = 3.37$.

SNA emerges [Fig. 7(d)]. We find that the higher is the order of the approximation, the more significant is the degree of the fractal structure of the attractor.

C. The fractal route

In fractal routes for the creation of SNAs, a torus attractor gets increasingly wrinkled and transforms into an SNA without the apparent mediation of any nearby unstable orbit. This generation mechanism of SNAs is independent of a bifurcation phenomenon.

We fix the parameter $\varepsilon = 3.1$ and let ω vary from 3.2 to 3.44. The other parameters and the initial values remain the same as Sec. III A. The attractors for successively larger ω are shown in Fig. 8. For $\omega = 3.2$, the attractor has one smooth branch, which indicates that the system is in a single torus state (1 T) [see Fig. 8(b)]. As ω increases, the attractor does not undergo torus-doubling bifurcation as in the last scenario. Instead, the branch of the attractor becomes irregular as shown in Figs. 8(c) and 8(d), but the attractor is continuous. In other words, the system is still in a torus state for

$\omega = 3.38$. When $\omega = 3.43$, the attractor becomes extremely wrinkled, and ultimately result is a strange attractor [see Figs. 8(e) and 8(f)]. Meanwhile, its maximum Lyapunov exponent is nonpositive [$\lambda \approx -0.00849$, see Fig. 9(a)]. Therefore, it is an SNA. For $\omega = 3.44$, the SNA is transformed into an attractor with a fractal structure and positive maximum Lyapunov exponent ($\lambda \approx 0.00458$), and, thus, the attractor [Fig. 8(g)] is chaotic.

In the fractal route, it is sometimes difficult to decide when the transition to SNAs occurs since the extremely wrinkled invariant curve looks very similar to an SNA. However, we can give a strict criterion by the phase sensitivity function. Figure 9(b) shows the time evolution of the maximum derivative, where the red and blue curves correspond to attractors as shown in Figs. 8(a) and 8(e), respectively. As the number of iterations increases, the derivative is not saturated after the transition to SNA, we infer that the derivative is not bounded. Therefore, the attractor shown in Fig. 8(e) is strange. To provide further evidence, the previous methods are also used to confirm the strange structure of SNA. We compute the scaling exponent ρ and present a reasonable power-law relationship

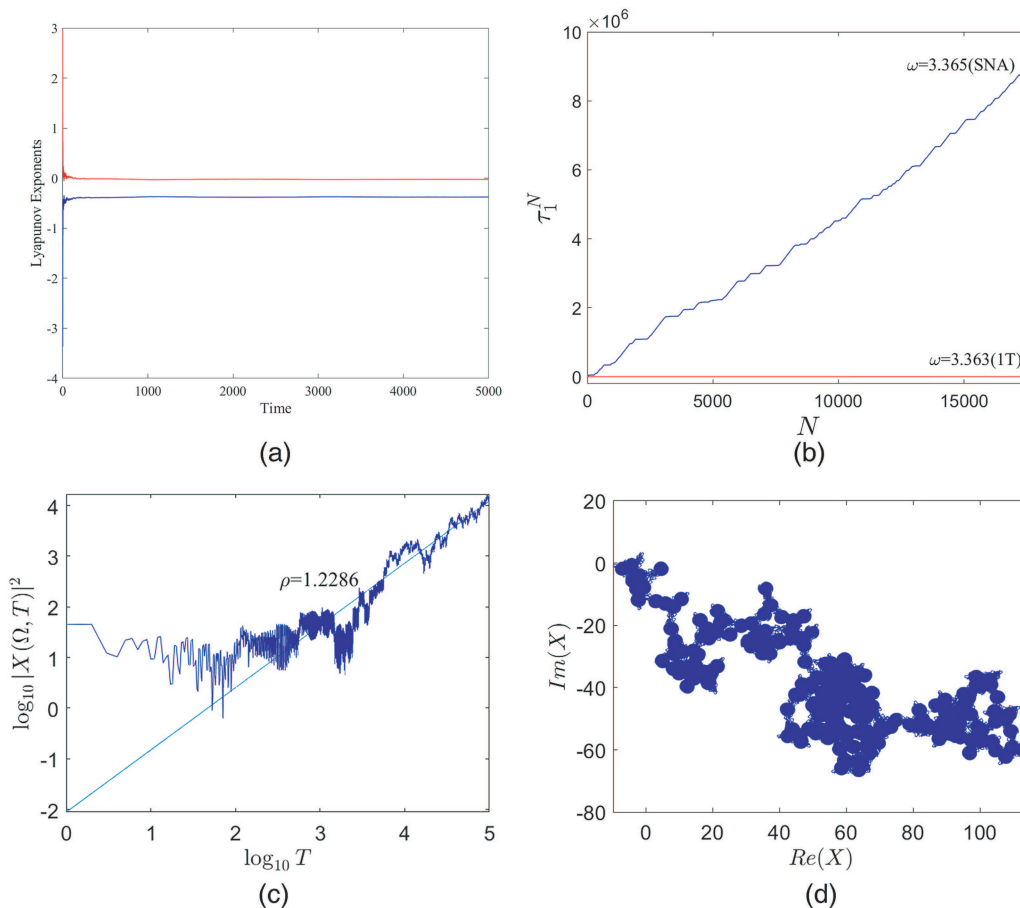


FIG. 11. For $\omega = 3.365$. (a) The entire Lyapunov spectrum. (b) The phase sensitivity exponent τ_1^N vs N , the 1 T for $\omega = 3.363$ (red line) and SNA for $\omega = 3.365$ (blue line). (c) The finite-time Fourier spectrum $X(\Omega, T)$ vs T in logarithmic scale. (d) The fractal walk in the complex plane (ReX, ImX).

$|X(\Omega, T)|^2 \sim T^{1.4540}$ and this behavior is shown in Fig. 9(c). Meanwhile, Fig. 9(d) demonstrates that the spectral trajectory in the complex plane (ReX, ImX) should exhibit a fractal behavior, as required for SNAs. To sum up, the attractor is an SNA.

D. The bubbling route

In addition to the route studied above, we also identified an uncommon route in a piecewise linear oscillator, called bubbling route (cf. Refs. 25 and 26) for the creation of SNAs. In this route, the torus quasiperiodic attractor forms local bubble-like structures in some regions and wrinkling of these under external force. However, the rest of the strands of the torus outside the bubbles remain largely unaffected. It is worth noting that this route is quite different from the well known fractal route, where the entire strands of the n -period torus continuously deform and become extremely wrinkled as the control parameters change.

To illustrate the emergence of bubbling route to SNAs in system (3), we fix the parameter $\varepsilon = 1.5$ and let the frequency ω vary from 3.36 to 3.37. The other parameters and the initial values remain

the same as Sec. III A. For $\omega = 3.363$, a 1T quasiperiodic attractor [Figs. 10(a) and 10(b)] occurs. As ω is increased to 3.3645, in the 1T quasiperiodic attractor appears bubble-like structures in the strand of the torus [see Figs. 10(c) and 10(d)]. These bubble-like structures are localized, namely, they occur on partial regions of the torus while the remaining part of the torus strand remains unaffected. As ω increases further to 3.365, the bubbles deform and become extremely wrinkled, which lead to the formation of an SNA [see Figs. 10(e) and 10(f)]. As ω continues to increase to 3.37, the SNA forms a 1-band chaotic attractor [Fig. 10(g)]. This transition process from a quasiperiodic attractor to an SNA via the bubbling route can be further verified by the entire Lyapunov spectrum [Fig. 11(a)], phase sensitivity function [Fig. 11(b)], and singular continuous spectrum analysis [Fig. 11(c)]: $\log_{10} |X(\Omega, T)|^2$ vs $\log_{10} T$, where $|X(\Omega, T)|^2 \sim T^{1.2286}$, and fractal trajectory in the complex plane (ReX, ImX) [Fig. 11(d)].

The mechanism of the bubbling route is that the quasiperiodic orbit gets increasingly unstable in its transverse direction as the control parameter ω changes, resulting in the formation of the bubble-like structures. This is reflected in Fig. 10(e), in partial regions of the torus.

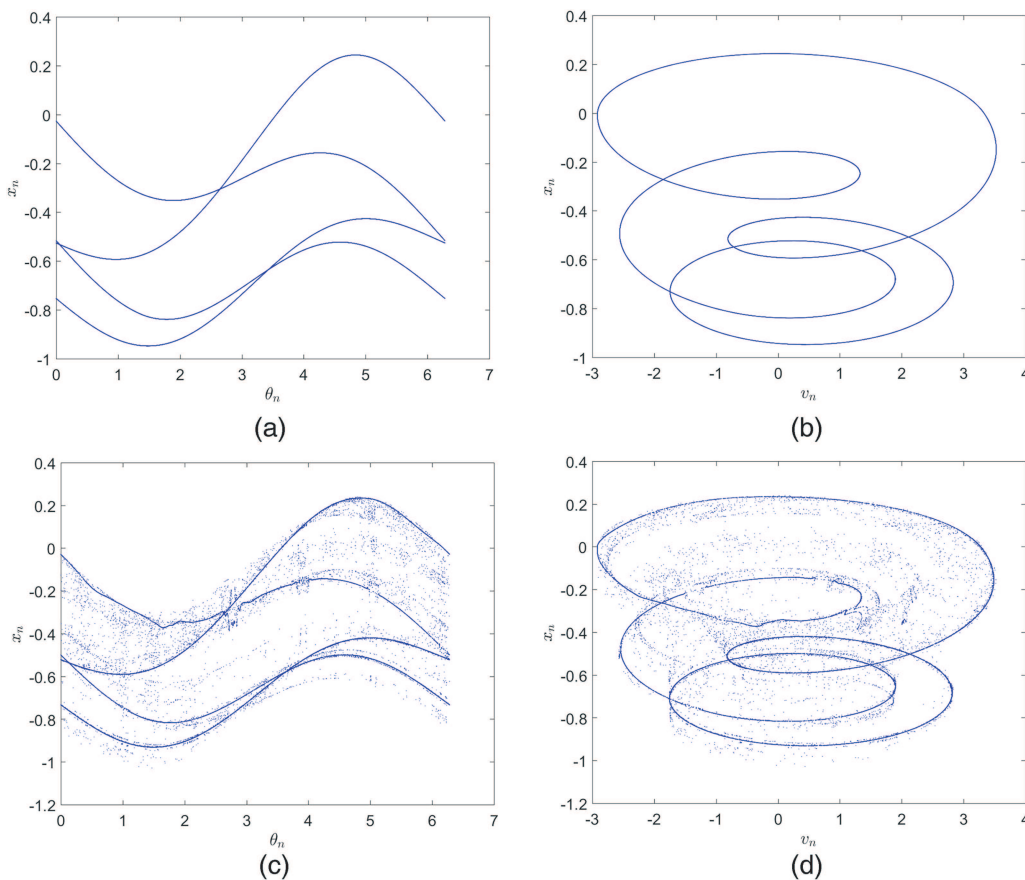


FIG. 12. For $\varepsilon = 0.1659095$, the phase diagrams of attractors in the (θ_n, x_n) -plane and (v_n, x_n) -plane: (a) and (b) $\omega = 9.995$, (c) and (d) $\omega = 10$.

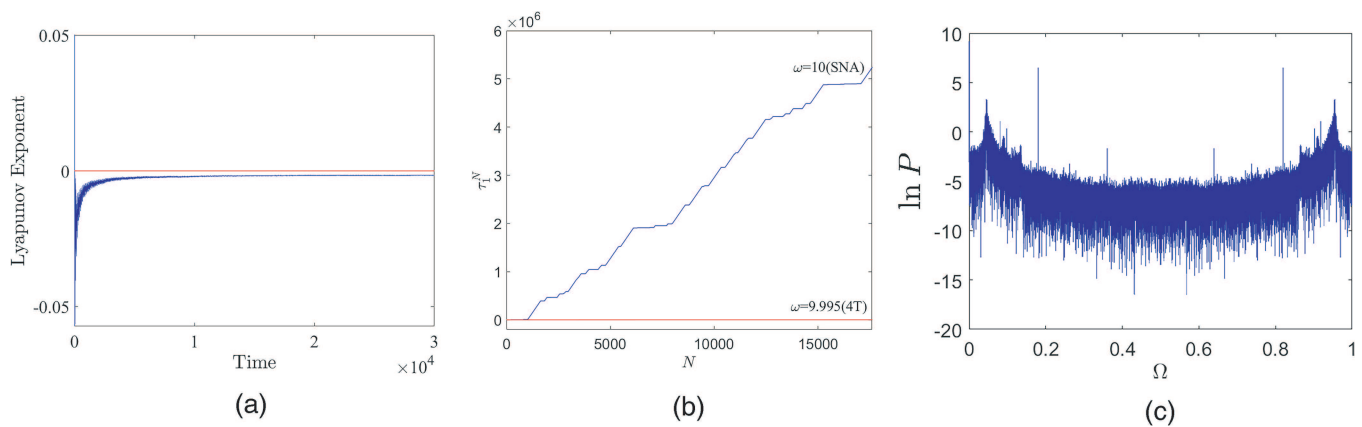


FIG. 13. For $\omega = 10$. (a) The maximum Lyapunov exponent. (b) The phase sensitivity exponent τ_1^N vs N , the 4T for $\omega = 9.995$ (red line) and SNA for $\omega = 10$ (blue line). (c) The singular continuous spectrum.

E. The type-I intermittency route

Intermittency routes can be the generation mechanisms for SNAs. We describe SNAs in terms of 4T torus intermittency, which is related to the saddle-node bifurcation. Let $\varepsilon = 0.165\,909\,5$ and the frequency ω vary from 9.995 to 10. For $\omega = 9.995$, the attractor is 4T quasiperiodic, as shown in Figs. 12(a) and 12(b). When ω is increased to 10, the approximate shape of the quasiperiodic orbit of the system is still present, but there are many disordered points near the orbit, which are characteristics of intermittency, as shown in Figs. 12(c) and 12(d). Here, the attractor is strange nonchaotic in Fig. 12(c). The nonchaotic property is denoted by the maximum Lyapunov exponent $\lambda \approx -0.001\,61$ [Fig. 13(a)]. The strange property of the attractor is characterized by the phase sensitivity [Fig. 13(b)] and the singular continuous spectrum [Fig. 13(c)].

V. CONCLUSIONS

Most of the research on strange nonchaotic dynamics focuses on smooth systems in different fields. In this work, the dynamics of a single-degree-of-freedom nonlinear oscillator under quasiperiodic excitation is considered. The complicated and interesting strange nonchaotic dynamics phenomena are revealed via the phase diagram, maximum Lyapunov exponent, singular continuous spectrum, phase sensitivity function, rational approximation, and so on. We demonstrate that the first scenario is torus-doubling bifurcation followed by the transition from the torus attractors to SNAs in such class of nonsmooth systems. The second is that the torus does not undergo a period-doubling cascade as controlling parameters vary, instead, the torus becomes extremely wrinkled, loses smoothness, and finally becomes fractal. The third is that the quasiperiodic attractor gets increasingly unstable in its transverse direction as the control parameter changes, resulting in the formation of bubble-like structures in partial regions of the torus, which eventually evolves into an SNA. The last one is that in the neighborhood of a saddle-node bifurcation many disordered points abruptly appear during the transition from 4T torus to SNA. The results of this work offer ideas

for the study of strange nonchaotic dynamics in nonsmooth systems as well as provide support for the design and optimization of devices in engineering fields.

ACKNOWLEDGMENTS

We sincerely thank the people who gave valuable comments. This paper was supported by the National Natural Science Foundation of China (NNSFC) (No. 12172306) and the Innovation Fund Project of Colleges and Universities in Gansu Province (No. 2021A-040).

AUTHOR DECLARATIONS

Conflict of Interest

The authors have no conflicts to disclose.

Author Contributions

Jicheng Duan: Writing – original draft (equal); Writing – review & editing (equal). **Wei Zhou:** Software (equal); Writing – original draft (equal). **Denghui Li:** Writing – original draft (equal). **Celso Grebogi:** Validation (equal).

DATA AVAILABILITY

The data that support the findings of this study are available from the corresponding author upon reasonable request.

REFERENCES

- 1C. Grebogi, E. Ott, S. Pelikan, and J. A. Yorke, “Strange attractors that are not chaotic,” *Physica D* **13**, 261–268 (1984).
- 2M. Ding, C. Grebogi, and E. Ott, “Evolution of attractors in quasiperiodically forced systems: From quasiperiodic to strange nonchaotic to chaotic,” *Phys. Rev. A* **39**, 2593–2598 (1989).
- 3A. S. Pikovsky and U. Feudel, “Characterizing strange nonchaotic attractors,” *Chaos* **5**, 253–260 (1995).

- ⁴T. Nishikawa and K. Kaneko, "Fractalization of a torus as a strange nonchaotic attractor," *Phys. Rev. E* **54**, 6114–6124 (1996).
- ⁵W. L. Ditto, M. L. Spano, H. T. Savage, S. N. Raueo, J. Heagy, and E. Ott, "Experimental observation of a strange nonchaotic attractor," *Phys. Rev. Lett.* **65**, 533 (1990).
- ⁶K. Thamilmaran, D. V. Senthilkumar, A. Venkatesan, and M. Lakshmanan, "Experimental realization of strange nonchaotic attractors in a quasiperiodically forced electronic circuit," *Phys. Rev. E* **74**, 036205 (2006).
- ⁷J. F. Lindner, V. Kohar, J. G. Learned, and W. L. Ditto, "Strange nonchaotic stars," *Phys. Rev. Lett.* **114**, 054–101 (2015).
- ⁸P. Glendinning, "Global attractors of pinched skew products," *Dyn. Syst.* **17**, 287–294 (2002).
- ⁹J. Stark, "Transitive sets for quasi-periodically forced monotone maps," *Dyn. Syst.* **18**, 351–364 (2003).
- ¹⁰P. Glendinning, T. Jäger, and G. Keller, "How chaotic are strange nonchaotic attractors," *Nonlinearity* **19**, 2005–2022 (2006).
- ¹¹G. Keller, "A note on strange nonchaotic attractors," *Fund. Math.* **151**, 139–148 (1996).
- ¹²M. Ding, C. Grebogi, and E. Ott, "Dimensions of strange nonchaotic attractors," *Phys. Lett. A* **137**, 167–172 (1989).
- ¹³G. Fuhrmann, M. Gröger, and T. Jäger, "Non-smooth saddle-node bifurcations II: Dimensions of strange attractors," *Ergod. Theory Dyn. Syst.* **30**, 2989–3011 (2018).
- ¹⁴Á. Haro and J. Puig, "Strange nonchaotic attractors in Harper maps," *Chaos* **16**, 033127 (2006).
- ¹⁵F. J. Romeiras and E. Ott, "Strange nonchaotic attractors of the damped pendulum with quasiperiodic forcing," *Phys. Rev. A* **35**, 4404–4413 (1987).
- ¹⁶A. Prasad, S. S. Negi, and R. Ramaswamy, "Strange nonchaotic attractors," *Int. J. Bifurcation Chaos* **11**, 291–309 (2001).
- ¹⁷U. Feudel, S. Kuznetsov, and A. S. Pikovsky, *Strange Nonchaotic Attractors: Dynamics between Order and Chaos in Quasiperiodically Forced Systems* (World Scientific Publishing Co. Pte. Ltd., Singapore, 2006), Chap. 6, pp. 75–127.
- ¹⁸G. Li, Y. Yue, J. Xie, and C. Grebogi, "Strange nonchaotic attractors in a non-smooth dynamical system," *Commun. Nonlinear Sci. Numer. Simul.* **78**, 104858 (2019).
- ¹⁹J. F. Heagy and S. M. Hammel, "The birth of strange nonchaotic attractors," *Physica D* **70**, 140–153 (1994).
- ²⁰Y. Zhang and G. Luo, "Torus-doubling bifurcations and strange nonchaotic attractors in a vibro-impact system," *J. Sound Vib.* **332**, 5462–5475 (2013).
- ²¹S. Datta, R. Ramaswamy, and A. Prasad, "Fractalization route to strange nonchaotic dynamics," *Phys. Rev. E* **70**, 046203 (2004).
- ²²A. Prasad, V. Mehra, and R. Ramaswamy, "Intermittency route to strange nonchaotic attractors," *Phys. Rev. Lett.* **79**, 4127–4130 (1997).
- ²³S. Y. Kim, W. Lim, and E. Ott, "Mechanism for the intermittent route to strange nonchaotic attractors," *Phys. Rev. E* **67**, 056203 (2013).
- ²⁴T. Yalçınkaya and Y. C. Lai, "Blowout bifurcation route to strange nonchaotic attractors," *Phys. Rev. Lett.* **77**, 5039–5042 (1996).
- ²⁵D. V. Senthilkumar, V. Srinivasan, K. Thamilmaran, and M. Lakshmanan, "Birth of strange nonchaotic attractors through formation and merging of bubbles in a quasiperiodically forced Chua's oscillator," *Phys. Rev. E* **78**, 066211 (2008).
- ²⁶K. Suresh, A. Prasad, and K. Thamilmaran, "Bubbling route to strange nonchaotic attractor in a nonlinear series LCR circuit with a nonsinusoidal force," *Phys. Lett. A* **377**, 612–621 (2013).
- ²⁷G. Li, Y. Yue, D. Li, J. Xie, and C. Grebogi, "The existence of strange nonchaotic attractors in the quasiperiodically forced Ricker family," *Chaos* **30**, 053124 (2020).
- ²⁸Y. Yue, P. Miao, and J. Xie, "Coexistence of strange nonchaotic attractors and a special mixed attractor caused by a new intermittency in a periodically driven vibro-impact system," *Nonlinear Dyn.* **87**, 1–21 (2017).
- ²⁹T. Cheng, Y. Zhang, and Y. Shen, "Infinite number of parameter regions with fractal nonchaotic attractors in a piecewise map," *Fractals* **29**, 2150087 (2021).
- ³⁰G. Li, Y. Yue, J. Xie, and C. Grebogi, "Multistability in a quasiperiodically forced piecewise smooth dynamical system," *Commun. Nonlinear Sci. Numer. Simul.* **84**, 105165 (2020).
- ³¹Y. Shen and Y. Zhang, "Mechanisms of strange nonchaotic attractors in a non-smooth system with border-collision bifurcations," *Nonlinear Dyn.* **96**, 1405–1428 (2019).
- ³²Y. Zhang and Y. Shen, "A new route to strange nonchaotic attractors in an interval map," *Int. J. Bifurcation Chaos* **30**, 2050063 (2020).
- ³³G. Li, Y. Yue, C. Grebogi, D. Li, and J. Xie, "Strange nonchaotic attractors and multistability in a two-degree-of-freedom quasiperiodically forced vibro-impact system," *Fractals* **29**, 2150103 (2021).
- ³⁴Y. Liu, Q. Wang, and H. Xu, "Bifurcations of periodic motion in a three-degree-of-freedom vibro-impact system with clearance," *Commun. Nonlinear Sci. Numer. Simul.* **48**, 1–17 (2017).
- ³⁵S. Kundu, S. Banerjee, J. Ing, E. Pavlovskaja, and M. Wiercigroch, "Singularities in soft-impacting systems," *Physica D* **241**, 553–565 (2012).
- ³⁶R. R. Aguiar and H. I. Weber, "Mathematical modeling and experimental investigation of an embedded vibro-impact system," *Nonlinear Dyn.* **65**, 317–334 (2011).
- ³⁷A. S. Pikovsky and U. Feudel, "Correlations and spectra of strange nonchaotic attractors," *J. Phys. A* **27**, 5209–5219 (1994).
- ³⁸A. H. Nayfeh and B. Balachandran, *Applied Nonlinear Dynamics* (John Wiley & Sons, Inc., New York, 1995).
- ³⁹S. M. Aravindh, A. Venkatesan, and M. Lakshmanan, "Strange nonchaotic attractors for computation," *Phys. Rev. E* **97**, 052212 (2018).